

Visualization of Motion and Geographic Characteristics of Bon Odori Dances in Akita Prefecture

Takeshi Miura (Graduate School of Engineering Science, Akita University)

Takeshi Shibata (College of Information and Systems, Muroran Institute of Technology)

Madoka Uemura (Faculty of Education and Human Studies, Akita University)

Katsubumi Tajima (Graduate School of Engineering Science, Akita University)

Hideo Tamamoto (Tohoku University of Community Service and Science)

Many folk dances have been passed down in Akita Prefecture, Japan. In particular, Bon Odori dances have attracted a great deal of attention. These dances have been passed down in respective regional communities, and each dance has been strongly affected by the geographic conditions of each region. In this study, we propose a map-deformation method to visualize the relationship between the regional motion-characteristic variation of Bon Odori dances in Akita Prefecture and the geographic elements of corresponding regions. This approach allows us to intuitively and easily comprehend the overview of the above relationship. Specifically, the motion characteristics of the dances investigated are first extracted by analyzing motion capture data of them. The motion-characteristic similarity of the dances is then evaluated based on the extracted motion-characteristic quantities. A deformed map having the form of a distance cartogram is finally constructed using the information on the above motion-characteristic similarity. The obtained distance cartogram suggested the influence of traffic networks on the transmission of the motion characteristics of the Bon Odori dances in Akita Prefecture, and the effectiveness of the map-deformation approach on visualizing the relationship between the regional motion-characteristic variation of folk dances and geographic elements.

1. Introduction

In Akita Prefecture, Japan, many folk dances have been passed down. In particular, *Bon Odori* dances have attracted a great deal of attention. These dances have been passed down in respective regional communities, and each dance has been strongly affected by the geographic and cultural conditions of each region [1]. By investigating their regional motion-characteristic variation and analyzing its relevance to the geographic elements of corresponding regions, therefore, the influence of surrounding geographic environment on the culture of a respective community may be clarified.

Using a technique of map deformation, i.e., constructing a cartogram, is known as one of the approaches to visualize geographically-referenced quantitative data [2]. As for the regional variation of folk dances, their motion characteristics can be extracted as geographically-referenced quantitative data by analyzing the motion capture (Mocap) data of them [3]. Consequently, it becomes possible to adopt a map-deformation approach to visualize the relationship between the regional motion-characteristic variation of folk dances and the geographic elements of corresponding regions. This allows us to intuitively and easily comprehend the overview of the above relationship.

Taking the above situation into account, we propose a method to visualize the relationship between the regional motion-characteristic variation of *Bon*

Odori dances in Akita Prefecture and the geographic elements of corresponding regions, using a map-deformation approach.

2. *Bon Odori* Dances of Akita Prefecture

The *Bon Odori* dances of Akita Prefecture have been classified into four groups: *Kazuno-Odori*, *Nanshū-Odori*, *Akita-Ondo* and *Yuri-Bon-Odori* Systems [4]. **Figure 1** shows the geographic distribution of the above groups (circles: settlements in which the *Bon Odori* dances investigated in this study have been passed down). **Table 1** shows the *Bon Odori* dances investigated in this study. Most of the dances belonging to the *Yuri-Bon-Odori* System have been lost until now. Therefore, we analyze only the dances belonging to the remaining three groups as shown in Table 1.

3. Map Deformation Based on Dance-motion Characteristics

3.1 Extraction of Dance-motion Characteristics

In Mocap data analysis to extract the motion characteristics of each dance, we adopt a method proposed in Ref [5]. This method provides motion-characteristic quantities in the form of a simple low-dimensional feature vector having only six components. This allows us to intuitively and easily grasp the motion characteristics of each Mocap data stream from the component values of the obtained feature vector. In addition, the similarity of Mocap data streams can be easily evaluated by calculating the

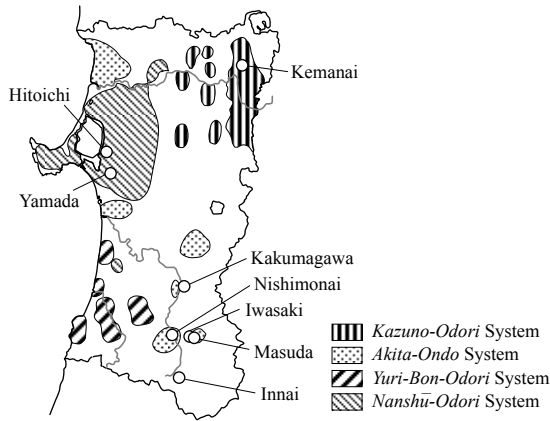


Fig. 1 Distribution of *Bon Odori* systems in Akita Prefecture (created by tracing the map on Page 17 of Ref. [4]).

Table 1 *Bon Odori* dances of Akita Prefecture

Group	Settlement	Dance	Mocap data (No., time)
Kazuno-Odori System	Kemanai	<i>Dainosaka</i>	3*, 10.8 s
		<i>Jinku</i>	3*, 9.9 s
Nanshū-Odori System	Hitoichi	<i>Dendenzuku</i>	3*, 6.6 s
		<i>Kitasaka</i>	6*, 5.5 s
	<i>Sankatsu</i>	4*, 11.6 s	
	Yamada	<i>Kitasaka</i>	5#, 5.5 s
		<i>Dagasuko</i>	4#, 6.9 s
Akita-Ondo System	Kubota	<i>Akita Ondo</i>	1*, 67.8 s
	Nakasen	<i>Donpan Odori</i>	1*, 33.8 s
		<i>Emazō Jinku</i>	1*, 32.7 s
	Kakumagawa	(no name)	1*, 59.3 s
	Nishimonai	<i>Ondo</i>	3*, 44.5 s
		<i>Ganke</i>	3*, 41.1 s
	Iwasaki	<i>Otoko Odori</i>	1*, 72.6 s
		<i>Onna Odori</i>	1*, 73.8 s
	Masuda	(no name)	2*, 69.2 s
	Innai	<i>Innai Ginzan Odori</i>	4*, 29.3 s
<i>Innai Ginzan Ondo</i>		2*, 39.3 s	

Mocap data: provided by Warabi-za Co., Ltd. (*) and the Center of Community (COC) Project of Akita University (*), time: mean time of all the Mocap data streams in a single dance.

distance between their feature vectors. In fact, the above feature vector shows a high classification performance comparable to other high-dimensional feature vectors (having over two hundred dimensions) in Mocap-data classification analysis [5].

The above six quantities are obtained by analyzing time-series data streams of the state variables representing the spatial arrangement of the body segments. Specifically, the body-segment spread along each of the axes of movement, i.e., frontal, vertical and sagittal axes [6], is formulated as a state variable, and evaluated by means of a phase plane analysis method [5] as follows.

First, a set of phase plane trajectories with respect to the temporal variation of the state variables $\sigma_x(n)$, $\sigma_y(n)$ and $\sigma_z(n)$ is drawn:

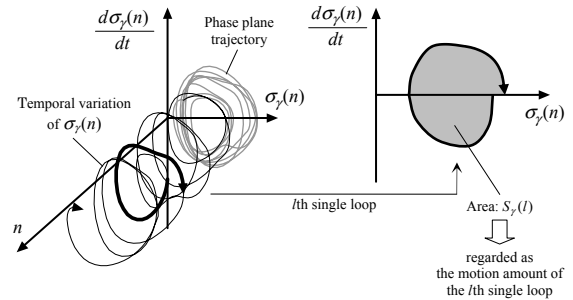


Fig. 2 Concept of phase plane analysis.

$$\sigma_\gamma(n) = \sqrt{\frac{1}{J} \sum_{j=1}^J \{p_{j,\gamma}(n) - \bar{p}_\gamma(n)\}^2} \quad (1)$$

$$\bar{p}_\gamma(n) = \frac{1}{J} \sum_{j=1}^J p_{j,\gamma}(n) \quad (\gamma: x, y \text{ or } z)$$

where $p_{j,\gamma}(n)$ is the γ -coordinate of the j th joint at the n th frame (coordinate system: fixed to the pelvis, x : leftward, y : upward and z : forward), J is the number of the principal joints used in the analysis (shoulders, elbows, wrists, fingers, hips, knees, ankles, toes, waist, neck and head, $J=19$). Each of $\sigma_x(n)$, $\sigma_y(n)$ and $\sigma_z(n)$ represents the amount of body-segment spread along each of the frontal, vertical and sagittal axes, respectively, at each instant. A phase plane consists of two axes (a state variable and its time derivative) [5], and the trajectories of $\sigma_x(n)$, $\sigma_y(n)$ and $\sigma_z(n)$ are drawn on their respective phase planes as shown in the left of Fig. 2. The time derivative of each state variable, $d\sigma_\gamma(n)/dt$, is numerically obtained by a finite-difference calculation [5], and the time series of $\sigma_\gamma(n)$ is filtered by a Gaussian filter (cut-off frequency: 10 Hz) before the finite-difference calculation to eliminate noise.

Next, two types of motion-characteristic quantities are extracted from the phase plane trajectories. The first type is a set of three quantities each of which represents the average motion amount in the γ -direction throughout the whole trajectory, and obtained as follows:

$$q_{MA\gamma} = \log \left\{ \frac{1}{L} \sum_{l=1}^L S_\gamma(l) + C \right\} \quad (\gamma: x, y \text{ or } z) \quad (2)$$

where L is the number of single loops included in the whole trajectory (Fig. 2), $S_\gamma(l)$ is the area of the l th single loop and C is a small constant to avoid $\log(0)$ (we set $C=e^{-10}$). Here, we define a locus from a negative-direction zero-cross point to the next point as a single loop as shown in Fig. 2. As a result, the greater the body-segment spread or the faster the motion speed, the larger the value of $q_{MA\gamma}$.

On the other hand, the second type is a set of three quantities each of which represents motion complexity in the γ -direction. This is quantified by using the value of approximate entropy [7], [8] as follows:

$$q_{MC\gamma} = \Phi^m - \Phi^{m+1} \quad (\gamma: x, y \text{ or } z) \quad (3)$$

$$\Phi^m = \frac{\sum_{n=1}^{N-(m-1)\tau_\gamma} \log D_n^m}{N - (m-1)\tau_\gamma}$$

$$D_n^m = \frac{\sum_{j=1}^{N-(m-1)\tau_\gamma} H(r - d(\mathbf{Z}_\gamma(n), \mathbf{Z}_\gamma(j)))}{N - (m-1)\tau_\gamma}$$

$$d(\mathbf{Z}_\gamma(n), \mathbf{Z}_\gamma(j)) = \max_{i=1,2,k=1,2,\dots,m} (|\mu_{i\gamma}(n + (k-1)\tau_\gamma) - \mu_{i\gamma}(j + (k-1)\tau_\gamma)|)$$

$$\mathbf{Z}_\gamma(n) = \begin{bmatrix} \mu_{1\gamma}(n) & \mu_{1\gamma}(n + \gamma_\gamma) \\ \mu_{2\gamma}(n) & \mu_{2\gamma}(n + \gamma_\gamma) \\ \dots & \mu_{1\gamma}(n + (m-1)\tau_\gamma) \\ \dots & \mu_{2\gamma}(n + (m-1)\tau_\gamma) \end{bmatrix}$$

where $\mu_{1\gamma}(n)$ and $\mu_{2\gamma}(n)$ are the standardized $\sigma_\gamma(n)$ and $d\sigma_\gamma(n)/dt$ (with zero mean and unity variance, standardized throughout the overall frames), N is the number of frames, $H(x)$ is the Heaviside function, and τ_γ is one fifth of the weighted mean of single-loop periods (weight: $S_\gamma(l)$ for each loop) obtained as follows:

$$\tau_\gamma = \text{round} \left[\frac{0.2}{\sum_{l=1}^L S_\gamma(l)} \times \sum_{l=1}^L \{S_\gamma(l)(n_{E\gamma}(l) - n_{S\gamma}(l) + 1)\} \right] \quad (4)$$

where $n_{S\gamma}(l)$ and $n_{E\gamma}(l)$ are the start and end frames of the l th γ -direction single loop, respectively. We set the parameters $m = 4$ and $r = 0.5$ according to Ref. [5]. The value of $q_{MC\gamma}$ becomes large when a trajectory on the phase plane shows a complex shape. In actual calculations, a fast algorithm [9] is used to reduce the calculation time.

As a result, the following six-dimensional feature vector is provided:

$$\mathbf{F} = [q_{MAx} \quad q_{MAy} \quad q_{MAz} \quad q_{MCx} \quad q_{MCy} \quad q_{MCz}]^T \quad (5)$$

where each of q_{MAx} , q_{MAy} and q_{MAz} is the average motion amount along each axis of movement (x : frontal, y : vertical and z : sagittal axes) and each of q_{MCx} , q_{MCy} and q_{MCz} is the motion complexity along each axis. The motion-characteristic similarity between two Mocap data streams can be evaluated by calculating the Euclidean distance between their feature vectors. In actual calculations, the component values of the feature vector are standardized

throughout the overall Mocap data streams used in the analysis (with zero mean and unity variance) to avoid underestimating (or overestimating) the variation of a particular component.

Each dance investigated in this study generally includes multiple Mocap data streams as shown in Table 1. In other words, each dance consists of a *set* of Mocap data streams. To evaluate similarity between dances, therefore, we use the Earth Mover's Distance (EMD) known as a representative between-set distance [10] as follows:

$$d_D(i, j) = \frac{\sum_{k_i=1}^{N_{D_i}} \sum_{l_j=1}^{N_{D_j}} d_M(k_i, l_j) u(k_i, l_j)}{\sum_{k_i=1}^{N_{D_i}} \sum_{l_j=1}^{N_{D_j}} u(k_i, l_j)} \quad (6)$$

where $d_D(i, j)$ is the distance between the i th and j th dances, $d_M(k_i, l_j)$ is the Euclidean distance between the feature vectors of the k_i th and l_j th Mocap data streams (k_i th: belonging to the i th dance, l_j th: to the j th dance), $u(k_i, l_j)$ is the ‘‘flow’’ from the k_i th Mocap data stream to the l_j th one (obtained by solving a transportation problem [10]), and N_{D_k} is the number of the Mocap data streams belonging to the k th dance. We solve the transportation problem under the following conditions:

$$\sum_{l_j=1}^{N_{D_j}} u(k_i, l_j) = \frac{1}{N_{D_i}}, \quad \sum_{k_i=1}^{N_{D_i}} u(k_i, l_j) = \frac{1}{N_{D_j}} \quad (7)$$

This means that every dance is evaluated with the same weighting, regardless of the difference in the Mocap-data-stream numbers of the respective dances.

3.2 Map Deformation

In the map-deformation process, a cartogram is constructed based on the motion characteristics of the investigated *Bon Odori* dances. Specifically, the positions of the settlements in which the dances have been passed down are changed in accordance with the motion-characteristic similarity of the dances. To evaluate the similarity between settlements from the motion-characteristic viewpoint, we again use the EMD as follows:

$$d_S(j, k) = \frac{\sum_{l_j=1}^{N_{S_j}} \sum_{m_k=1}^{N_{S_k}} d_D(l_j, m_k) u(l_j, m_k)}{\sum_{l_j=1}^{N_{S_j}} \sum_{m_k=1}^{N_{S_k}} u(l_j, m_k)} \quad (8)$$

where $d_S(j, k)$ is the distance between the j th and k th settlements, $d_D(l_j, m_k)$ is the distance between the l_j th and m_k th dances (l_j th: belonging to the j th settlement, m_k th: to the k th settlement), $u(l_j, m_k)$ is the ‘‘flow’’ from the l_j th dance to the m_k th one, and N_{S_i} is the number of the dances belonging to the l th settlement. To eliminate the influence of difference in the numbers of the dances in the respective settlements,

we use the “flow” values obtained under the following conditions:

$$\sum_{m_k=1}^{N_{S_k}} u(l_j, m_k) = \frac{1}{N_{S_j}}, \quad \sum_{l_j=1}^{N_{S_j}} u(l_j, m_k) = \frac{1}{N_{S_k}} \quad (9)$$

The positions of the settlements can be determined by applying a distance cartogram construction algorithm to the obtained set of between-settlement distances. We use an algorithm proposed in Ref. [11] as shown below.

Figure 3 shows the algorithm. First, the values of the following parameters are inputted: $x_G(i)$, $y_G(i)$ (coordinates of the i th settlement in the original geographic map, $x_G(i)$ for the horizontal axis and $y_G(i)$ for the vertical axis^{*1}, $1 \leq i \leq N_S$, N_S : number of settlements), $d_S(j, k)$ (distance between the j th and k th settlements, $j, k \in C_S$, C_S : set of settlement links taken into account), and $w(j, k)$ (weight of the link between the j th and k th settlements, $j, k \in C_S$, set by users). Next, the bearing angle between the j th and k th settlements in the cartogram, $\theta'(j, k)$, is calculated ($j, k \in C_S$, the value in the original geographic map obtained below is used as the initial value):

$$\begin{aligned} \sin \theta'(j, k) &= \frac{x_G(j) - x_G(k)}{d_G(j, k)} \\ \cos \theta'(j, k) &= \frac{y_G(j) - y_G(k)}{d_G(j, k)} \\ d_G(j, k) &= \sqrt{\{x_G(j) - x_G(k)\}^2 + \{y_G(j) - y_G(k)\}^2} \end{aligned} \quad (10)$$

Then, the coordinate values of the settlements in the cartogram ($x_C(i)$ and $y_C(i)$, $1 \leq i \leq N_S$) are obtained by iterations of the following linear least squares optimizations and the renewal of the $\theta'(j, k)$ values:

$$\text{Minimize } \sum_{j, k \in C} [w(j, k) \{d_S(j, k) \sin \theta'(j, k) - (x_C(j) - x_C(k))\}]^2 \quad (11)$$

$$\text{Minimize } \sum_{j, k \in C} [w(j, k) \{d_S(j, k) \cos \theta'(j, k) - (y_C(j) - y_C(k))\}]^2 \quad (12)$$

$$\begin{aligned} \sin \theta(j, k) &= \frac{x_C(j) - x_C(k)}{d_C(j, k)} \\ \cos \theta(j, k) &= \frac{y_C(j) - y_C(k)}{d_C(j, k)} \\ d_C(j, k) &= \sqrt{\{x_C(j) - x_C(k)\}^2 + \{y_C(j) - y_C(k)\}^2} \end{aligned}$$

*1 Note that the roles of the variables x and y in this study is contrary to those in the Japanese surveying and mapping community (x : northing, y : easting) [12]. We assign x and y the horizontal and vertical axes, respectively, in accordance with mathematical conventions.

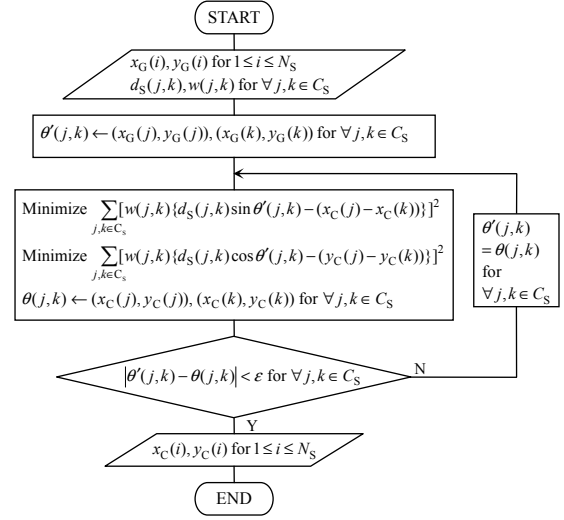


Fig. 3 Algorithm for distance cartogram construction.

where $\theta(j, k)$ is the renewed $\theta'(j, k)$. In Eqs. (11) and (12), the squared errors between the actual distances in the cartogram ($x_C(j) - x_C(k)$ and $y_C(j) - y_C(k)$) and the target values ($d_S(j, k) \sin \theta'(j, k)$ and $d_S(j, k) \cos \theta'(j, k)$) are minimized at every axis (this type of least squares problems can be numerically solved by singular value decomposition [13]).

After the convergence of the iteration loop (determined by the condition $|\theta'(j, k) - \theta(j, k)| < \varepsilon$ for all $j, k \in C_S$, ε : parameter for determining the convergence of iteration), the obtained $x_C(i)$ and $y_C(i)$ values are outputted. As a result of applying the above algorithm, a deformed map having the form of a distance cartogram is provided.

As for geographic elements such as roads, rivers, lakes and boundary lines between prefectures, their positions are determined by the Delaunay triangulation and barycentric interpolation [14]. In the triangulation process, the positions of the settlements are used as vertices of triangles.

4. Results and Discussion

This section describes details of the obtained results. To execute the map-deformation algorithm mentioned in the Section 3.2, a user must select settlement links taken into account in advance. **Table 2** shows the selected settlement links and their weight values. The settlement links corresponding to the roads each of which gives a direct link between a settlement pair (13 links) are selected with the weight value $w(j, k) = 1.0$. To consider the relationship between the group of the *Kazuno-Odori* System and that of the *Akita-Ondo* System between which no direct connection exists, the link between the *Kemanai* and

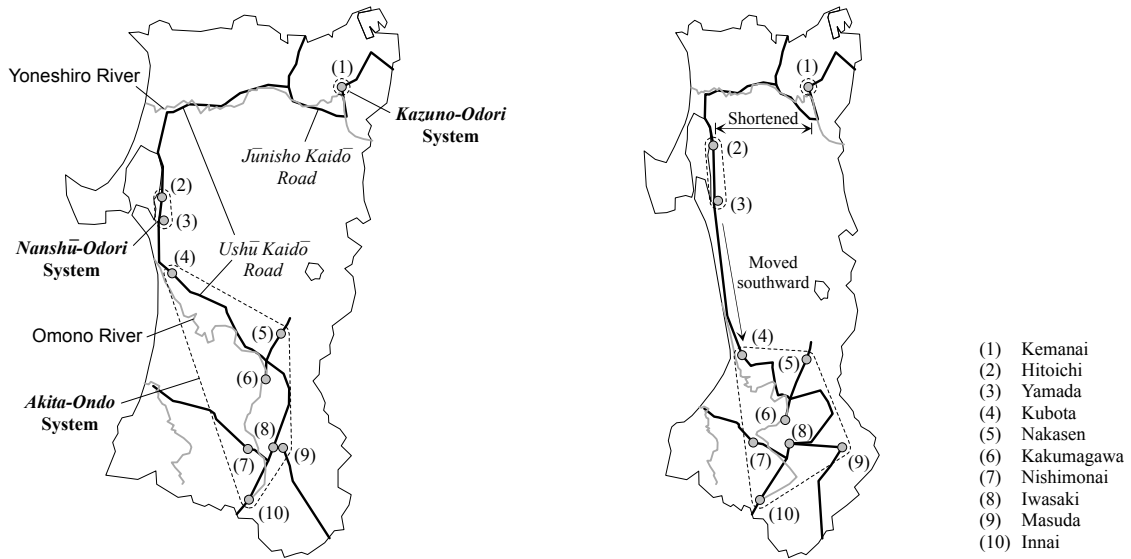


Fig. 4 Comparison between the original geographic map of Akita Prefecture (left) and the distance cartogram (right).

Table 2 Settlement links considered in map deformation.

Weight	Link
1.0	Kemanai – Hitoichi
	Hitoichi – Yamada
	Yamada – Kubota
	Kubota – Nakasen
	Kubota – Kakumagawa
	Kubota – Iwasaki
	Nakasen – Kakumagawa
	Nakasen – Iwasaki
	Kakumagawa – Iwasaki
	Nishimonai – Iwasaki
	Nishimonai – Innai
	Iwasaki – Masuda
	Iwasaki – Innai
	0.02

Nakasen settlements is weighted with a small value ($w(j, k)=0.02$).

Figure 4 shows the comparison between the original geographic map of Akita Prefecture and the obtained distance cartogram. Two distinctive features with respect to map deformation are seen in the cartogram. One is the shortening of the distance between the Kazuno-Odori and Nanshu-Odori Systems, and the other is a remarkable southward movement of the Kubota settlement. One can notice that both are related to the shortening of the road-river dual-path route*2 (former: Ushu Kaido and Junisho Kaido Roads and Yoneshiro River, latter: Ushu Kaido Road and Omono River). This suggests the influence of traffic networks on the transmission of dance-motion characteristics.

Figure 5 shows the scatter plot of the motion-characteristic distribution of the dances investi-

gated in this study. This is obtained by applying a technique of metric multidimensional scaling [15] to the set of EMDs of all the dance pairs. Arrows in the scatter plot are the axes of the motion-characteristic quantities obtained by using correlation coefficients between the components of the scatter plot and the quantities of the Mocap data streams as follows:

$$A_F = R_{q_1, q_2}^F \frac{[r_{F, q_1}^{q_2} \quad r_{F, q_2}^{q_1}]^T}{|[r_{F, q_1}^{q_2} \quad r_{F, q_2}^{q_1}]^T|} \quad (14)$$

where A_F is the vector representing the direction and magnitude of the axis of the quantity F , q_1 and q_2 are the components of the horizontal and vertical axes of the scatter plot, R_{q_1, q_2}^F is the multiple correlation coefficient between F and a set of q_1 and q_2 , and $r_{F, a}^b$ is the partial correlation coefficient between F and the variable a holding the variable b fixed.

It is seen in Fig. 5 that the dances of the Akita-Ondo System commonly show a high motion-complexity characteristic. This community is thought to contribute to the southward movement of the Kubota settlement in the cartogram and the concentration of the Akita-Ondo dances into an area smaller than that in the original geographic map. As for the Kazuno-Odori and Nanshu-Odori Systems, on the other hand, the characteristic of showing simplicity in dance motion is commonly seen in Fig. 5. This might have caused the shortening of the distance between them in the cartogram.

The obtained cartogram effectively visualized the correlation between the above motion-characteristic variation of Bon Odori dances and the geographic elements, e.g., traffic networks, of Akita Prefecture. However, the motion-characteristic quantities ex-

*2 In the early-modern times, most of the rivers in Akita Prefecture were used as water routes.

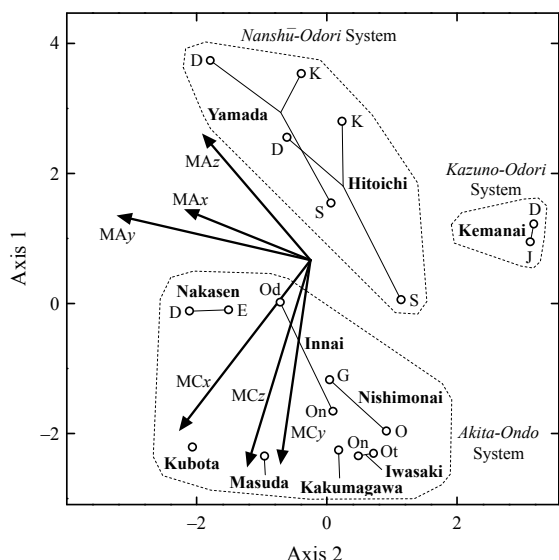


Fig. 5 Motion-characteristic distribution of the *Bon Odori* dances of Akita Prefecture. Arrow: axis of the motion-characteristic quantity (MA: motion amount, MC: motion complexity).

tracted from Mocap data are limited to those representing only two types of motion characteristics, i.e., motion amount and motion complexity. To examine the validity of the proposed method, therefore, additional work is needed to compare with cases in which more various types of information on motion characteristics are provided.

5. Conclusion

In this study, the effectiveness of the map-deformation approach on visualizing the relationship between the regional motion-characteristic variation of *Bon Odori* dances in Akita Prefecture and the geographic elements of corresponding regions was demonstrated to a certain extent. To confirm the limitation of the proposed approach will be the subject of future work.

Acknowledgments This study was supported by JSPS Grants-in-Aid for Scientific Research (KAKENHI) Grant Number JP18K11981.

References

[1] Mimuro, K.: An Introduction to a Study on the Traditional Folk Dance of Japan –With Special Reference to Traditional Folk Dances in the Kibi District–, *Bulletin of School of Education, Okayama University*, Vol.18, pp.154-173 (1964)

(in Japanese).
 [2] Han, R., Li, Z., Ti, P. and Xu, Z.: Experimental Evaluation of the Usability of Cartogram for Representation of GlobeLand30 Data, *Int. J. Geo-Inf.*, Vol.6-180, pp.1-13 (2017).
 [3] Miura, T., Kaiga, T., Katsura, H., Shibata, T., Tajima, K. and Tamamoto, H.: Quantitative Motion Analysis of the Japanese Folk Dance “Hitoichi Bon Odori,” *IPSP Symposium Series*, Vol.2013, No.4, pp.167-174 (2013).
 [4] Japan Broadcasting Corporation, ed.: *Tōhoku Min’yōshū Akita Ken (A Collection of Folk Songs of Tōhoku Region: Akita Prefecture)*, Japan Broadcast Publishing Association (1957) (in Japanese).
 [5] Miura, T., Kaiga, T., Shibata, T., Tajima, K. and Tamamoto, H.: Low-dimensional Feature Vector Extraction from Motion Capture Data by Phase Plane Analysis, *Journal of Information Processing*, Vol.25, pp.884-887 (2017).
 [6] Bartlett, R.: *Introduction to Sports Biomechanics*, 2nd ed., Routledge (2007).
 [7] Pincus, S.M.: Approximate Entropy as a Measure of System Complexity, *Proc. Natl. Acad. Sci. USA*, Vol.88, pp. 2297–2301 (1991).
 [8] Kaffashi, F., Foglyano, R., Wilson, C.G. and Loparo, K.A.: The Effect of Time Delay on Approximate & Sample Entropy Calculations, *Physica D*, Vol.237, No.23, pp. 3069–3074 (2008).
 [9] Manis, G.: Fast Computation of Approximate Entropy, *Computer Methods and Programs in Biomedicine*, Vol.91, No.1, pp. 48–54 (2008).
 [10] Rubner, Y., Tomasi, C. and Guibas, L.J.: The Earth Mover’s Distance as a Metric for Image Retrieval, *International Journal of Computer Vision*, Vol.40, No.2, pp. 99–121 (2000).
 [11] Shimizu, E. and Inoue, R.: A New Algorithm for Distance Cartogram Construction, *International Journal of Geographical Information Science*, Vol.23, No.11, pp.1453-1470 (2009).
 [12] Okazawa, H., Kubodera, T., Sasada, K., Tasumi, M., Hosokawa, Y., Matsuo, E. and Mihara, M.: *Newer Surveying -Fundamentals and Applications with Newest Technology-*, Corona Publishing Co., Ltd. (2014) (in Japanese).
 [13] Press, W.H., Teukolsky, S.A., Vetterling, W.T. and Flannery, B.P.: *Numerical Recipes in C: The Art of Scientific Computing*, 2nd ed., Cambridge University Press (1992).
 [14] Bies, S. and van Kreveld, M.: Time-Space Maps from Triangulations, Didimo, W. and Patrignani, M. (Eds.): *GD 2012, LNCS 7704*, pp.511-516 (2013).
 [15] Hair, Jr., J.F., Black, W.C., Babin, B.J. and Anderson, R.E.: *Multivariate Data Analysis*, 7th ed. Pearson Education Inc. (2010).